PAPER

In vitro evaluation of Schiff base-decorated phthalocyanines for photodynamic therapy in PC3 prostate cancer cells

Nagihan Kocaağa,[a] Ayşegül Türkkol,[b] Ceren Can Karanlık, ![ID] *[a,c]
Mehmet Dinçer Bilgin[b] and Ali Erdoğmuş*[a,c]

Schiff base-decorated non-ionic phthalocyanine compounds with different metals and a metal-free derivative were synthesized and characterized using different spectroscopic techniques. The influence of the central metal on the photophysicochemical properties was systematically investigated in DMSO. The obtained results reveal that the singlet oxygen quantum yield followed the order **In3b** > **Zn3b** > **3bH₂Pc** in DMSO. The synthesized non-ionic phthalocyanine compounds, except metal-free phthalocyanine (0.12 for **3bH₂Pc**), have good Φ_Δ values (0.71 for **Zn3b** and 0.85 for **In3b**) compared with the unsubstituted ZnPc in DMSO (Φ_Δ = 0.67). In addition to the photophysicochemical studies, *in vitro* PDT studies were also performed on PC3 prostate cancer cells to evaluate the biological activity of Pcs. All compounds exhibited low dark cytotoxicity at the selected concentration. Upon light irradiation, phthalocyanine-mediated PDT significantly reduced cell viability and induced apoptotic cell death. These effects were accompanied by a pronounced increase in intracellular ROS generation, particularly in the cells treated with metallophthalocyanine-mediated PDT. In particular, **In3b**- and **Zn3b**-mediated PDT exhibited markedly enhanced cytotoxic and apoptotic effects compared with metal-free **3bH₂Pc**. These findings demonstrate a strong correlation between improved photophysical properties, increased ROS generation, and enhanced *in vitro* PDT efficacy.

1. Introduction

Cancer, a disease with multistep processes, is one of the most life-threatening diseases affecting humans. According to GLOBOCAN data, lung cancer was estimated to have caused the greatest number of cancer-related deaths in 2023.[1] Photodynamic therapy (PDT), which is a non-invasive and laser-controlled cancer treatment method, has been successfully applied to different cancer cell types, such as prostate cancer,[2] breast cancer,[3] colon cancer,[4] lung cancer[5] and melanoma.[6] The three main components necessary for PDT application are molecular oxygen, photosensitizer and light. In PDT, malignant tumors are destroyed with reactive oxygen species (ROS), which are obtained as a result of photochemical reactions.[7,8] Lipophilic phthalocyanines (Pcs), that are planar and aromatic and are derived by the linking of different substituents and metals, provide various distinct properties. Due to these properties, suitable phthalocyanines have been syn-

thesized and used for numerous applications like catalysis, gas sensors, photodynamic therapy, electrochromism, liquid crystal, and solar cells.[9–15] The presence of diamagnetic metals, such as Zn(II), Al(III), Ga(III), Mg(II) and In(III), in the central cavity of phthalocyanine compounds increases the generation of singlet oxygen and the triplet lifetime.[16–20] Schiff bases, also called imines, which play an essential role in coordination chemistry, are synthesized by the formation of an azomethine bond (–N=CH–) as a result of the condensation reaction between carbonyl compounds and primary amines. These types of compounds are extensively employed in pharmaceutical and biological sciences owing to their diverse chemical and biological properties. Among the biological properties, their pronounced antitumoral activity makes them attractive candidates for anticancer applications, particularly in photodynamic therapy (PDT).[21–28]

While phthalocyanines are well-known photosensitizers with strong absorption in the therapeutic window and efficient singlet oxygen generation, Schiff base moieties contribute additional electronic modulation and intrinsic biological activity. Furthermore, the incorporation of diamagnetic metal ions, such as Zn(II) and In(III), can promote intersystem crossing and improve triplet state formation, thereby enhancing the generation of reactive oxygen species. Therefore, the design of imine-functionalized metal-free and metallophthalocyanines

[a]Department of Chemistry, Yildiz Technical University, 34220 Esenler, Istanbul, Turkey. E-mail: aerdog@yildiz.edu.tr
[b]Aydın Adnan Menderes University, Faculty of Medicine, Department of Biophysics, 09010 Aydın, Turkey
[c]Health Biotechnology Joint Research and Application Center of Excellence, 34220 Istanbul, Turkey

provides a promising platform for the development of advanced PDT agents.

In this study, novel metal-free and metallophthalocyanines (Zn(II) and In(III)) bearing imine segments were successfully synthesized and comprehensively characterized for the first time. Their photophysicochemical properties, including fluorescence, singlet oxygen generation, and photodegradation quantum yields, were systematically investigated in DMSO. By directly correlating these photophysicochemical parameters with *in vitro* PDT results, the present work provides a comprehensive evaluation of imine-substituted metal-free and metallophthalocyanines. The comparative analysis clearly demonstrates the critical role of the central metal ion in determining the PDT efficiency, offering valuable insights for the rational design of imine-based photosensitizers with improved therapeutic performance.

2. Experimental

The synthetic pathway for the new peripherally Schiff base-decorated phthalocyanine complexes (**3bH₂Pc**, **Zn3b** and **In3b**) is shown in Scheme 1. The Schiff base derivative **3a** was syn-thesized *via* a condensation reaction between 4-methoxybenzaldehyde and 4-aminophenol using acetic acid as a catalyst. After that, **3a** reacted with 4-nitrophthalonitrile under basic conditions to yield the phthalonitrile derivative **3b**. Schiff base-decorated complexes (**3bH₂Pc**, **Zn3b** and **In3b**) were obtained by the tetramerization of the phthalonitrile derivative **3b** with related metal salts in the presence of a DBU catalyst.

2.1. Synthesis of 4-[(*E*)-{[4-methoxyphenyl]methylidene}amino]phenol (3a)

Compound **3a** was synthesized by using the method reported in the literature.[29] A solution of 2 mL of 4-methoxybenzaldehyde was added to a solution of 4-aminophenol (1.045 g, 9.5 mmol) in 12.5 mL dry ethanol in a two-necked round-bottomed flask. After adding 5 drops of glacial acetic acid, the mixture was refluxed at 78 °C for 3.5 hours under an argon atmosphere. The obtained white product was filtered and washed with cold methanol, followed by drying the precipitate in a vacuum over P_2O_5. **Yield:** 1.56 g (71%). **M.P.:** 188 °C–189 °C. **Anal. calc. for $C_{14}H_{13}NO_2$ (%):** C, 73.99; H, 5.77; N, 6.16. Found (%): C, 73.96, H, 5.79, N, 6.12. **FT-IR ν_{max}/cm^{-1}:** 3058 (Ar–CH), 2979–2847 (Aliph. –CH), 1604 (C=N), 1510,
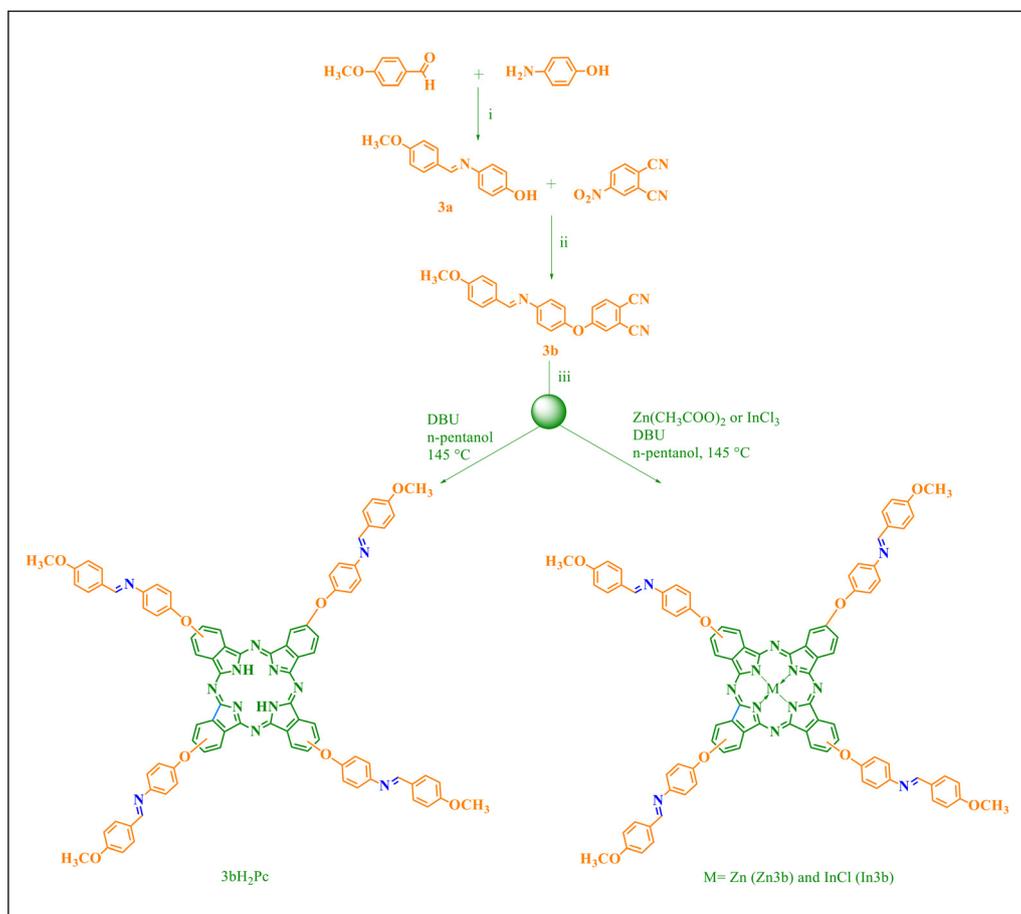
Scheme 1 Synthetic pathway of the imine-substituted phthalocyanines (**3bH₂Pc**, **Zn3b**, and **In3b**): (i) dry ethanol and glacial acetic acid at 78 °C; (ii) K_2CO_3 and dry DMF at 60 °C and (iii) no metal salt for **3bH₂Pc**, Zn(Ac)₂ for **Zn3b**, and InCl₃ for **In3b**, *n*-pentanol, and DBU at 145 °C.

1447 (C=C). **^{1}H-NMR (CDCl$_3$), (δ: ppm)** = 9.82 (s, 1 Ar–OH), 8.57 (s, 1 HC=N), 7.78 (d, $J \approx$ 8.7 Hz; 2 Ar–H), 7.40 (d, $J \approx$ 7.0 Hz; 2 Ar–H), 7.07 (d, $J \approx$ 7.7 Hz; 2 Ar–H), 6.75 (d, $J \approx$ 8.8 Hz; 2 Ar–H), 3.83 (s, 3H, O–CH$_3$). **MS (MALDI-MS) m/z:** calc. 227.26; found: 227.088 [M]$^+$.

2.2. Synthesis of 4-{4-[(E)-{[4-methoxyphenyl]methylidene}amino]phenoxy}benzene-1,2-dicarbonitrile (3b)

The Schiff base ligand (**3a**) (1.29 g, 5.7 mmol) and 12.5 mL dry DMF were dissolved in a two-necked round-bottomed flask. After adding the solution of 4-nitrophthalonitrile (0.98 g, 5.7 mmol) to 6 mL dry DMF, the mixture was stirred for 20 min at 60 °C. Anhydrous potassium carbonate (1.61 g, 11.6 mmol) was added portion-wise to the reaction mixture for two hours under an argon atmosphere. The reaction mixture was stirred for 24 hours at 60 °C under an argon atmosphere. At the end of the reaction, the mixture was poured into a 500 mL ice-water (50 : 50) solution and collected by centrifugation. The collected precipitate was crystallized in acetone and washed with cold acetone. Then, the pure product was dried under vacuum over P$_2$O$_5$. **Yield:** 1.25 g (62%). **M.P.:** 152 °C–153 °C. **Anal. calc. for C$_{22}$H$_{15}$N$_3$O$_2$ (%):** C, 74.78; H, 4.28; N, 11.89. Found (%): C, 74.80, H, 4.25, N, 11.84. **FT-IR ν_{max}/cm^{-1}:** 3077 (Ar–H), 2971–2839 (Aliph. C–H), 2230 (C≡N), 1600 (C=N), 1567, 1508, 1481 (C=C), 1284, 1090 (C–O–C). **^{1}H-NMR (500 MHz, CDCl$_3$):** δ (ppm) = 8.44 (s, 1 H–C=N), 7.90 (d, $J \approx$ 7.6 Hz; 2 Ar–H), 7.75 (d, $J \approx$ 8.7 Hz; 1 Ar–H), 7.32–7.27 (m, 4 Ar–H), 7.12 (d, $J \approx$ 8.5 Hz; 2 Ar–H), 7.03 (d, $J \approx$ 8.5 Hz; 2 Ar–H), 3.92 (s, 3H, CH$_3$). **^{13}C-NMR (126 MHz, CDCl$_3$):** δ (ppm) = 162.57, 162.06, 160.33, 151.14, 150.56, 135.43, 130.69, 128.94, 122.97, 121.38, 121.37, 121.28, 117.69, 115.42, 114.99, 114.32, 108.76, 55.50. **MS (MALDI-MS) m/z:** calc. 353.37; found: 353.02 [M]$^+$.

2.3. General synthesis method of the phthalocyanine compounds (3bH$_2$Pc, Zn3b, and In3b)

A mixture of compound **3b** (0.11 g, 0.31 mmol for **3bH$_2$Pc** and 0.10 g, 0.29 mmol for **Zn3b** and **In3b**), metal salt (0.017 g, 0.07 mmol anhydrous zinc(II) acetate and indium(III) chloride for **Zn3b** and **In3b**, respectively) and 3 drops of DBU in n-pentanol (3 mL) was stirred at 145 °C for 5 h under argon atmosphere in a Schlenk tube. Metal salt was not used in the synthesis of metal-free phthalocyanine (**3bH$_2$Pc**). When the reaction mixture was cooled to room temperature, it was precipitated using 200 mL n-hexane and then centrifuged. Subsequently, the crude product obtained was purified by column chromatography on silica gel using THF as the eluent.

2.3.1. 2(3),9(10),16(17),23(24)-Tetrakis-4-{4-[(E)-{[4-methoxyphenyl]methylidene}amino]phenoxy} phthalocyanine (3bH$_2$Pc). Yield: 0.093 g (21%). Anal. calc. for C$_{88}$H$_{62}$N$_{12}$O$_8$ (%): C, 74.67; H, 4.41; N, 11.87. Found (%): C, 74.59, H, 4.38, N, 11.82. **UV-vis (DMSO) λ_{max}/nm (log ε):** 703 (3.56), 674 (3.61), 641 (3.38), 333 (4.53). **FT-IR ν_{max}/cm^{-1}:** 3288 (–NH), 3065 (Ar–H), 2930, 2858 (Aliph. C–H), 1602 (C=N), 1226, 1025 (C–O–C). **^{1}H-NMR (DMSO-d$_6$), (δ: ppm)** = 8.6 (s, 4 HC=N), 8.7–6.6 (m, 44 Ar–H), 3.84 (s, 12 H, 4 CH$_3$). **MS (MALDI-MS) m/z:** calc. 1415.51; found: 1415.20 [M]$^+$.

2.3.2. 2(3),9(10),16(17),23(24)-Tetrakis-4-{4-[(E)-{[4-methoxyphenyl]methylidene}amino]phenoxy} phthalocyaninato zinc (II) (Zn3b). Yield: 0.08 g (19%). Anal. calc. for C$_{88}$H$_{60}$N$_{12}$O$_8$Zn (%): C, 71.47; H, 4.09; N, 11.37. Found (%): C, 71.18, H, 4.03, N, 11.30. **UV-vis (DMSO) λ_{max}/nm (log ε):** 682 (4.80), 615 (4.14), 348 (4.66). **FT-IR ν_{max}/cm^{-1}:** 3062 (Ar–H), 2929, 2839 (Aliph. C–H), 1603 (C=N), 1226, 1089 (C–O–C); **^{1}H-NMR (DMSO-d$_6$), (δ: ppm)** = 8.8–6.8 (m, 4 HC=N, 44 Ar–H), 3.84 (s, 12 H, 4 CH$_3$). **MS (MALDI-MS) m/z:** calc. 1478.87; found: 1478.944 [M]$^+$.

2.3.3. 2(3),9(10),16(17),23(24)-Tetrakis-4-{4-[(E)-{[4-methoxyphenyl]methylidene}amino]phenoxy} phthalocyaninato chloroindium(III) (In3b). Yield: 0.037 g (8%). Anal. calc. for C$_{88}$H$_{60}$N$_{12}$O$_8$InCl (%): C, 67.59; H, 3.87; N, 10.75. Found (%): C, 67.32, H, 3.79, N, 10.74. **UV-vis (DMSO) λ_{max}/nm (log ε):** 696 (4.16), 624 (3.95), 340 (4.34). **FT-IR ν_{max}/cm^{-1}:** 3063 (Ar–H), 2930, 2864 (Aliph. C–H), 1602 (C=N), 1224, 1080 (C–O–C). **^{1}H-NMR (DMSO-d$_6$), (δ: ppm)** = 8.58 (s, 4 HC=N), 7.9–6.6 (m, 44 Ar–H), 3.84 (s, 12 H, 4 CH$_3$). **MS (MALDI-MS) m/z:** calc. 1563.76; found: 1526.35 [M − Cl − 2H]$^+$.

3. Results and discussion

3.1. Synthesis and characterization

Compound **3a** was synthesized via the condensation reaction between 4-aminophenol and 4-methoxybenzaldehyde. In the presence of K$_2$CO$_3$, the starting phthalonitrile compound (**3b**) was synthesized via the nucleophilic aromatic substitution reaction between **3a** and 4-nitrophthalonitrile in basic media (DMF). Afterwards, a metal-free phthalocyanine compound was obtained with the cyclotetramerization of phthalonitrile compound **3b** in n-pentanol and DBU. Unlike the metal-free phthalocyanine, the synthesis of **Zn3b** and **In3b** was carried out in the presence of Zn(CH$_3$COO)$_2$ and InCl$_3$, respectively. UV-vis, FT-IR, ^{1}H-NMR, MALDI-TOF and elemental analysis techniques were used to characterize the structures of all the synthesized novel compounds. The synthetic routes of **3a**, **3b**, **3bH$_2$Pc**, **Zn3b** and **In3b** are given in Scheme 1.

In the FT-IR spectrum of compound **3a**, the azomethine (–C=N) peak was observed at 1604 cm^{-1}. The C≡N and C=N vibrations at 2230 and 1600 cm^{-1}, respectively, were observed upon the formation of the phthalonitrile compound **3b**. After the cyclotetramerization of phthalonitrile, the disappearance of the specific C≡N vibration confirms the synthesis of **3bH$_2$Pc**, **Zn3b** and **In3b** complexes. Also, the observed peak at 3288 cm^{-1} corresponds to the specific inner core –NH band of compound **3bH$_2$Pc**. Furthermore, Ar–H, aliphatic C–H, C=N and C–O–C vibration bands of all the synthesized phthalocyanine compounds were observed at expected frequencies (Fig. S7, S10, S13 using compound **3bH$_2$Pc**, **Zn3b** and **In3b**, as examples, respectively).

As shown in the ^{1}H-NMR spectrum of compound **3a**, the signal corresponding to the HC=N group was observed at 8.57 ppm. Although **3a** shows a proton signal of aromatic –OH

at 9.82 ppm, this peak disappeared with the synthesis of **3b**. The obtained proton signals of the HC=N group were seen at 8.6 ppm for **3bH₂Pc** and 8.58 ppm for **In3b**. Also, aromatic –CH and proton signals of HC=N for **Zn3b** were obtained at 8.8–6.8 ppm. Aliphatic proton signals were found at 3.84 for **3bH₂Pc**, **Zn3b** and **In3b** (Fig. S2, S4, S9 and S12 using compounds **3a**, **3b**, **Zn3b** and **In3b** as an example, respectively). In the mass spectra, molecular ion peaks were observed at 227.088 $[M]^+$, 353.02 $[M]^+$, 1415.20 $[M]^+$, 1478.944 $[M]^+$ and 1526.35 $[M - Cl - 2H]^+$ for **3a**, **3b**, **3bH₂Pc**, **Zn3b** and **In3b**, respectively (Fig. S1, S3, S6, S8 and S11 using compound **3a**, **3b**, **3bH₂Pc**, **Zn3b** and **In3b** as an example, respectively).

3.2. Ground state electronic absorption spectra

Phthalocyanines exhibit two typical major bands, which are based on electronic transitions, like n–π* and π–π* transitions. Metallophthalocyanines and dihydrogen phthalocyanines, also called metal-free phthalocyanines, have the D_{4h} and D_{2h} symmetry, respectively. Due to these different symmetries, when metal-free Pcs exhibit two characteristic Q (Q_x and Q_y) bands, metallophthalocyanines exhibit one strong Q band in the UV-vis spectra. The Q bands are observed at 703 and 674 nm for **3bH₂Pc**, 682 nm for **Zn3b** and 696 nm for **In3b** in DMSO. Because of the substitution of 4-{4-[(E)-{[4-methoxyphenyl] methylidene}amino]phenoxy} moieties on the Pc ring, the Q bands of compounds **3bH₂Pc**, **Zn3b** and **In3b** were red-shifted in contrast to the unsubstituted ZnPc (672 nm) in DMSO. The electronic absorption spectra of all synthesized phthalocyanines are given in Fig. 1.

Aggregation significantly influences the photodynamic activity of phthalocyanines, leading to strong π–π stacking interactions, which reduce light absorption efficiency, suppress excited-state lifetimes, and cause decreased singlet oxygen generation. Therefore, the aggregation behavior of the synthesized non-ionic phthalocyanines was determined by measuring the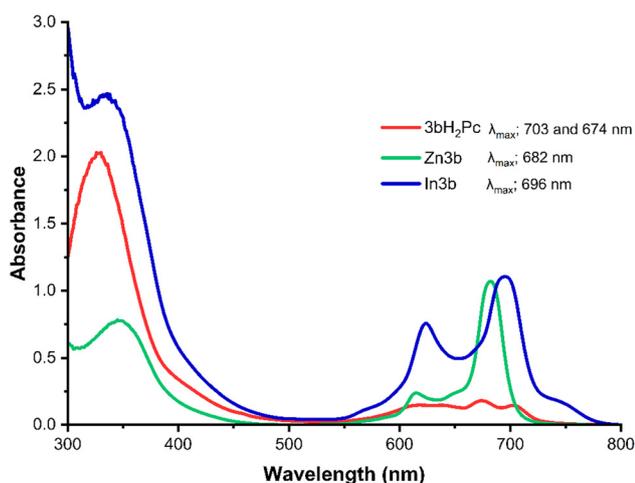 absorbance values of solutions prepared at different molarities in DMSO. These measurements indicated that the synthesized imine-substituted non-ionic phthalocyanines did not show any aggregation in DMSO. Moreover, the concentrations ranging from 1×10^{-5} to 5×10^{-5} M for **3bH₂Pc**, 2×10^{-6} to 10×10^{-6} M for **Zn3b** and 2×10^{-5} to 6×10^{-5} M for **In3b** in DMSO obey the Lambert-Beer law (Fig. 2 and Fig. S14 in the SI).

3.3. Photophysicochemical yields

3.3.1. Fluorescence spectra and quantum yields. The fluorescence spectra of imine-substituted non-ionic phthalocyanines (**3bH₂Pc**, **Zn3b**, and **In3b**) were investigated in DMSO. The excitation spectra of all synthesized metal-free and metallophthalocyanines were similar to the absorption spectra and both spectra were mirror images of the emission spectra. The fluorescence emission maxima were determined at 713 nm for **3bH₂Pc**, 695 nm for **Zn3b** and 712 nm for **In3b**. The observed data from absorption, emission and excitation spectra are listed in Table 1 (Fig. 1 and 3).

The fluorescence quantum yields (Φ_F) of imine-substituted phthalocyanines are listed in Table 2. The Φ_F values (10^{-2}) of **3bH₂Pc**, **Zn3b** and **In3b** were determined as 1.7, 12.2 and 0.52, respectively. When compared with the Φ_F value of unsubstituted ZnPc (0.18), all synthesized imine-substituted phthalocyanines have lower Φ_F values in DMSO. Also, compound **In3b** has the lowest Φ_F value because of the heavy atom effect of the indium ion. Compared with amino-substituted structures,[30–33] the presence of methoxy substituents is not sufficient to acti-
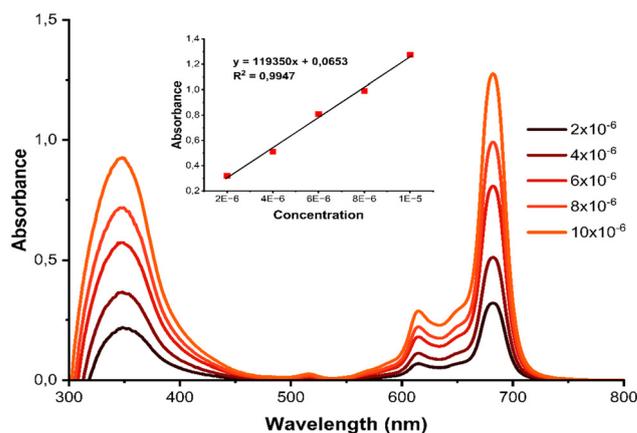

Fig. 2 Absorbance changes of **Zn3b** in DMSO at different concentrations ranging from 2×10^{-6} to 10×10^{-6} M.

Fig. 1 Electronic absorption spectra of the non-ionic phthalocyanine compounds (**3bH₂Pc**, **Zn3b**, and **In3b**) in DMSO.

Table 1 Absorption, excitation and emission spectral data for the non-ionic phthalocyanine compounds in DMSO

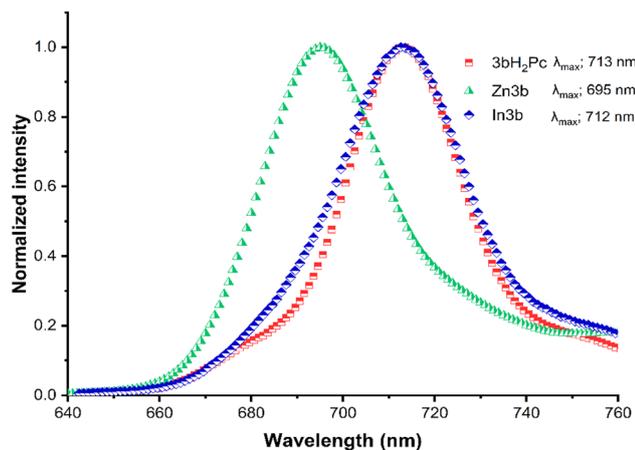| Compound	Q band λ_{max} (nm)	log ε	Excitation λ_{Ex} (nm)	Emission λ_{Em} (nm)	Stokes shift
3bH₂Pc	703 and 674	3.56 and 3.61	705	713	10
Zn3b	682	4.80	684	695	13
In3b	696	4.16	705	712	16

Fig. 3 Emission spectra of the **3bH$_2$Pc**, **Zn3b** and **In3b** compounds in DMSO.

Table 2 Fluorescence, singlet oxygen and photodegradation quantum yields of the non-ionic phthalocyanine compounds in DMSO

Compound	Φ_F (10^{-2}) DMSO	Φ_d (10^{-4}) DMSO	Φ_Δ DMSO
3bH$_2$Pc	1.7	0.7	0.12
Zn3b	12.2	28.0	0.71
In3b	0.52	3.0	0.85

vate the photoinduced electron transfer (PET) process. Consequently, methoxy-substituted **3bH$_2$Pc**, **Zn3b** and **In3b** exhibit higher fluorescence quantum yields.

3.3.2. Singlet oxygen quantum yields. Singlet oxygen, which destroys cancerous tissue as a result of its reaction with biomolecules, is one of the most important parameters examined in determining the effectiveness of PDT. Singlet oxygen generation is strongly influenced by both solvent properties and structural features of the photosensitizer. The imine functionality is further substituted with a methoxy (–OCH$_3$) group, which is known to act as an electron-donating substituent through resonance. The presence of the methoxy group increases the electron density on the imine moiety and contributes to the extension of the π-conjugated framework of the phthalocyanine. This increased electron density may facilitate charge transfer within the excited state, which can enhance ISC processes.[34,35] Solvent polarity also plays a critical role in modulating the ISC. Polar solvents may facilitate ISC and enhance triplet state population, thereby improving singlet oxygen quantum yields.[19,36,37]

In the present study, photophysicochemical measurements were performed in DMSO, a highly polar aprotic solvent known for its strong solvation ability and relatively high oxygen solubility. Moreover, as an aprotic solvent, DMSO does not form strong hydrogen-bonding interactions with the macrocycle, thereby minimizing specific solvent–solute interactions that could otherwise alter the intrinsic electronic properties of the phthalocyanine core. The solution, with non-ionic phthalocyanines containing 1,3-diphenylisobenzofuran

(DPBF) as a quencher in DMSO, was irradiated with light every 5 s. The change in the absorbance of DPBF (417 nm) was monitored using the UV-vis spectra. The obtained spectra for Schiff base-decorated metal-free and metallophthalocyanines are given in Fig. 4 and Fig. S15, and the values are listed in Table 2. The Φ_Δ values were calculated as 0.12 for **3bH$_2$Pc**, 0.71 for **Zn3b** and 0.85 for **In3b** in DMSO. The metal-free **3bH$_2$Pc** exhibits a lower Φ_Δ value than the unsubstituted ZnPc (0.67) in DMSO, whereas **In3b** has the highest Φ_Δ value among all the investigated phthalocyanines. These enhancements arise from the strong heavy atom effect[38] of the indium ion,[39] which significantly facilitates intersystem crossing (ISC) and consequently singlet oxygen generation. In recent studies, the synthesized non-ionic phthalocyanines have similar Φ_Δ values compared with the other studied metal-free and metallophthalocyanines containing imine groups in DMSO.[28,40,41] Also, several studies have demonstrated that the incorporation of imine functional groups into π-conjugated systems can positively influence ISC processes and consequently, enhance singlet oxygen quantum yields. The presence of the imine linkage contributes to the extension and modulation of the conjugated electronic framework, altering the distribution of frontier molecular orbitals and facilitating more efficient population of the triplet excited state. In addition, the lone pair electrons on the nitrogen atom may participate in n → π* transitions, which are known to promote spin–orbit coupling and improve ISC efficiency.[28,42,43]

3.3.3. Photodegradation quantum yields. Photodegradation studies, which yield necessary parameters for maintaining the activity of phthalocyanine and keeping the drug concentration constant, were conducted for determining the stability of phthalocyanines under light irradiation. Stable compounds have photodegradation quantum yields (Φ_d) in the order of 10^{-3} to 10^{-6}, as reported in the literature.[44–46] Fig. 5 and Fig. S16 in the SI display the Φ_d spectra of imine-substituted phthalocyanines. The Φ_d values calculated from the spectra given in Fig. 5 and Fig. S16 in the SI are listed in
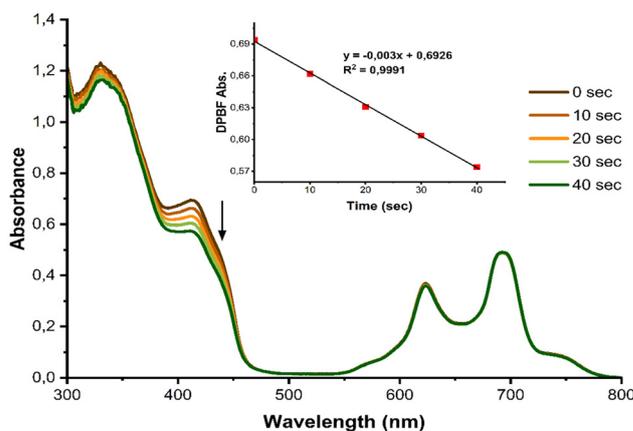

Fig. 4 Typical spectrum for the determination of singlet oxygen quantum yield of the **In3b** compound in DMSO using DPBF as a singlet oxygen quencher.
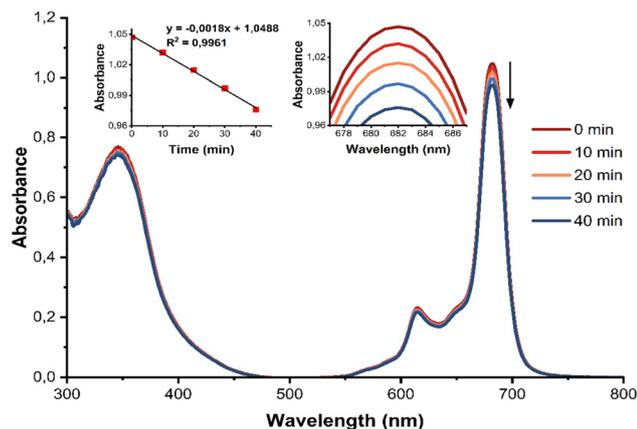
Fig. 5 Typical spectrum for the determination of photodegradation of the **Zn3b** compound in DMSO.

Table 2. The Φ_d values of all synthesized imine substituted non-ionic phthalocyanines indicate in the order of 10^{-3} in DMSO. These results show that compounds **3bH₂Pc**, **Zn3b** and **In3b** have sufficient stability. Also, **Zn3b** is the most unstable compound in DMSO.

3.4. *In vitro* studies

3.4.1. Cytotoxicity assessment. Based on the MTT assay results, a concentration of 5 μM was identified as the highest concentration that did not induce a statistically significant cytotoxic effect compared with the control group for **Zn3b**, **In3b**, and **3bH₂Pc**. Therefore, this concentration was selected as the treatment dose for subsequent experiments (Fig. 6).

3.4.2. Effects of PDT on cell viability and apoptosis. Following PDT, cell viability decreased to 83.17% ± SEM in the **3bH₂Pc**-mediated PDT group, 38.83% ± SEM in the **In3b**-mediated PDT group, and 48.48% ± SEM in the **Zn3b**-mediated PDT group. All phthalocyanine-mediated PDT treatments resulted in a statistically significant reduction in cell viability compared with the control group ($p < 0.05$) (Fig. 7).

PDT mediated by different phthalocyanine derivatives resulted in varying levels of total apoptosis in PC3 cells. Following the **3bH₂Pc**-mediated PDT, total apoptosis was observed at 5.08%, whereas **In3b**-mediated PDT induced a marked increase in total apoptosis to 46.27%, and **Zn3b**-mediated PDT resulted in 40.20% total apoptosis. All phthalocyanine-mediated PDT treatments led to a statistically significant increase in total apoptosis compared with the control group ($p < 0.05$). The apoptosis results are presented in Fig. 8.
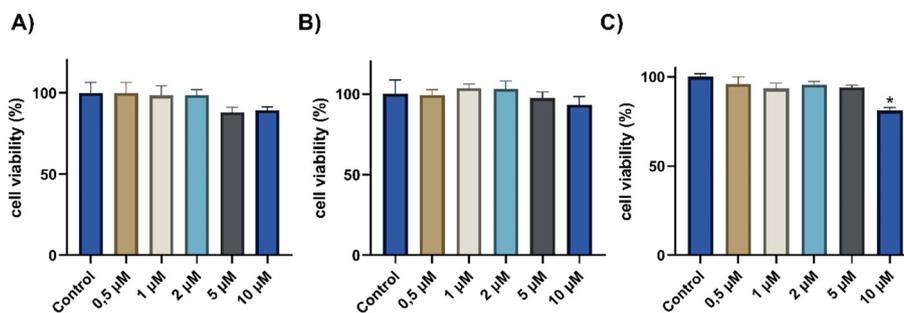

Fig. 6 Dose-dependent MTT cytotoxicity analysis of the phthalocyanine derivatives in PC3 cells: (A) **3bH₂Pc**, (B) **In3b**, and (C) **Zn3b**. Data are presented as column graphs. Statistically significant differences compared with the control group are indicated by * ($p < 0.05$).
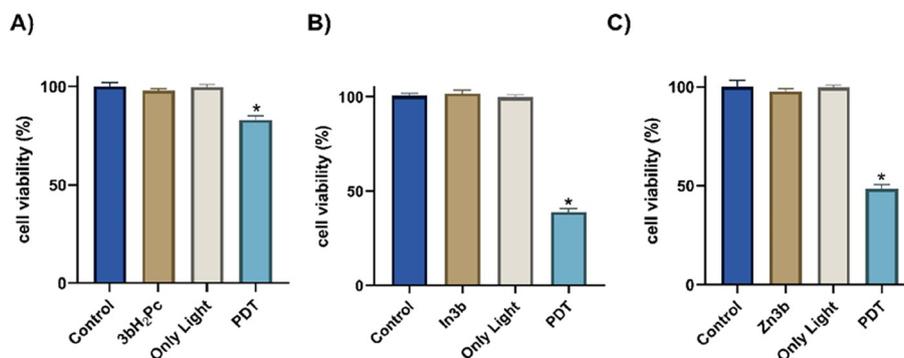

Fig. 7 MTT assay results following PDT in PC3 cells: (A) **3bH₂Pc**-mediated PDT, (B) **In3b**-mediated PDT, and (C) **Zn3b**-mediated PDT. The phthalocyanine derivatives were applied at a concentration of 5 μM. Data are presented as column graphs. Statistically significant differences compared with the control group are indicated by * ($p < 0.05$).
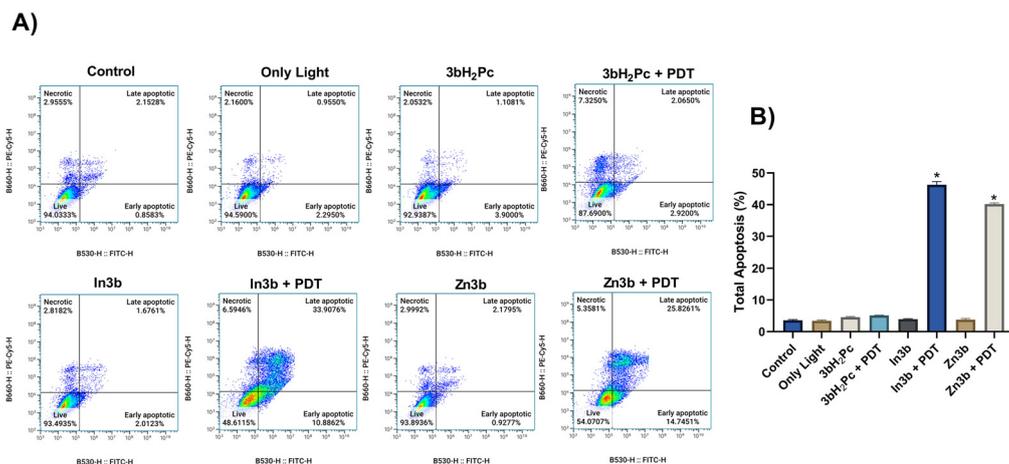
Fig. 8 Apoptosis analysis following PDT in PC3 cells. (A) Representative flow cytometry dot plots showing Annexin V-FITC/PI staining after phthalocyanine-mediated PDT. (B) Quantitative analysis of the total apoptosis. Data are presented as column graphs and expressed as mean $\pm$ SEM ($n = 3$). Statistically significant differences compared with the control group are indicated by * ($p < 0.05$).
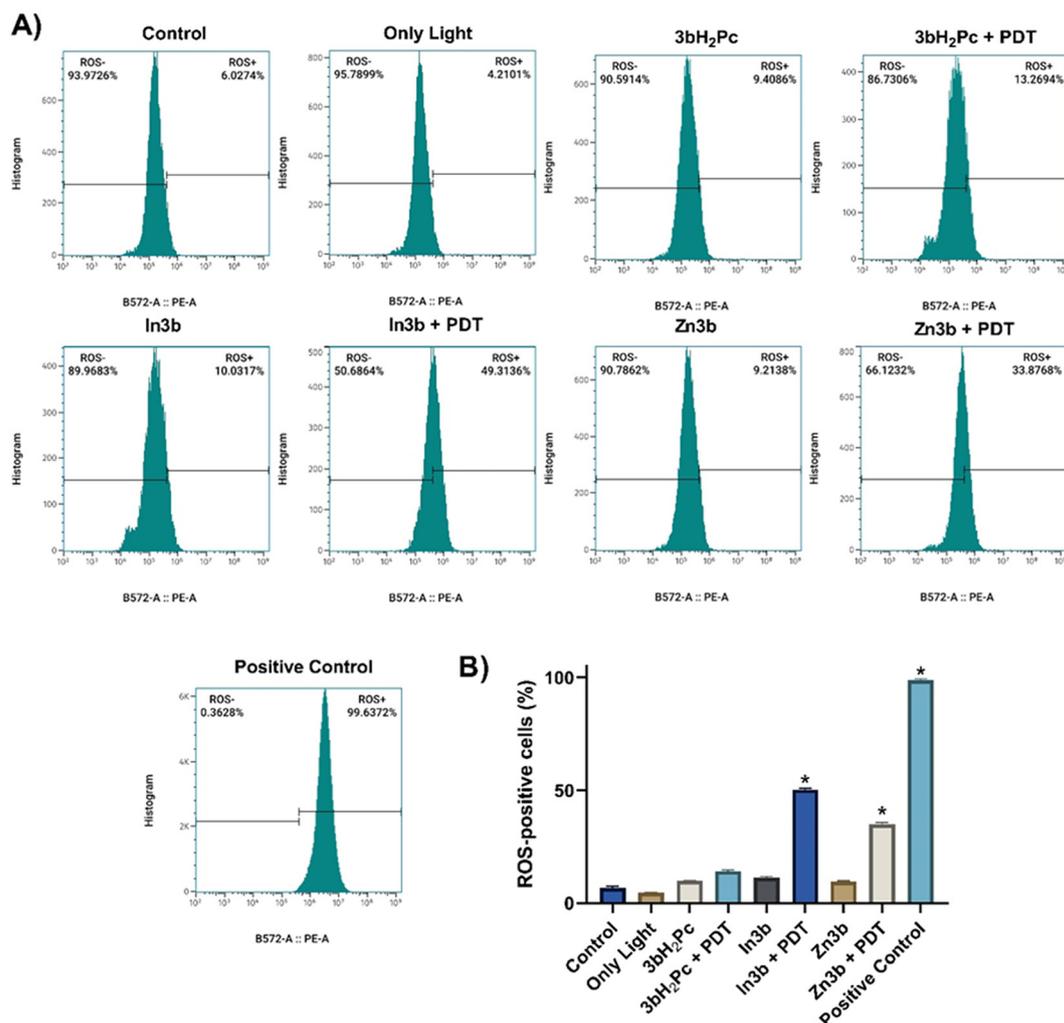

Fig. 9 Phthalocyanine-mediated PDT-induced intracellular ROS generation in PC3 cells. (A) Representative flow cytometry fluorescence histograms showing rightward shifts in the DHE fluorescence intensity (x-axis shift) following photodynamic therapy (PDT). (B) Quantitative analysis of ROS-positive cells (%), presented as column graphs. Data are expressed as mean $\pm$ SEM. Statistically significant differences compared with the control group are indicated by * ($p < 0.05$). *tert*-Butyl hydroperoxide (*t*BHP) was used as a positive control.

3.4.3. Effect of phthalocyanine-mediated PDT on cellular ROS levels. The DHE-based flow cytometric analysis revealed a marked increase in intracellular ROS levels in PC3 cells following phthalocyanine-mediated PDT (Fig. 9).

Quantitative evaluation demonstrated that **3bH₂Pc**-mediated PDT resulted in a modest elevation of ROS-positive cells to 13.26%, whereas a pronounced increase was observed in cells treated with **In3b**-mediated PDT (49.31%) and **Zn3b**-mediated PDT (33.87%).

Consistent with the cytotoxicity and apoptosis data, metallophthalocyanines, particularly **In3b**, induced substantially higher ROS levels than the metal-free derivative, highlighting the critical role of the central metal ion in enhancing PDT efficacy. The elevated ROS production correlated well with the observed reductions in cell viability and enhancements in total apoptosis, supporting a ROS-mediated mechanism of cell death in PC3 cells following PDT.

In this study, the photodynamic effects of the imine-substituted metal-free and metallophthalocyanines (**3bH₂Pc**, **Zn3b**, and **In3b**) were further evaluated through *in vitro* biological assays. Although the Φ_d values of all Schiff base-substituted phthalocyanines were reported to be comparable, the presence of a central metal ion was shown to significantly enhance Φ_Δ, particularly in the **In3b** derivative due to the heavy atom effect. This photophysical advantage was clearly reflected in the biological outcomes observed in the present study.

Consistent with their favorable photophysical properties, all phthalocyanine derivatives exhibited minimal dark cytotoxicity at the selected concentration of 5 μM, confirming their suitability as photosensitizers for PDT. Upon light irradiation, a significant reduction in cell viability was observed in all phthalocyanine-mediated PDT groups, indicating effective photodynamic activation. Notably, **In3b**- and **Zn3b**-mediated PDT resulted in a markedly stronger decrease in cell viability compared with **3bH₂Pc**-mediated PDT, which correlates well with the enhanced singlet oxygen generation associated with the presence of metal ions in the phthalocyanine core.[47,48]

The analysis of apoptosis data further supported these findings, revealing a pronounced increase in total apoptotic cell death following **In3b**- and **Zn3b**-mediated PDT. The significantly higher apoptosis rates induced by these metallophthalocyanines suggest that metal-assisted enhancement of intersystem crossing and singlet oxygen production plays a critical role in triggering programmed cell death pathways.[49] In contrast, the relatively lower apoptotic effect observed for **3bH₂Pc** may be attributed to the absence of a central metal ion, resulting in reduced ROS generation despite comparable Φ_d values.[50]

4. Conclusions

In this work, novel imine-substituted metal-free and metallophthalocyanines were successfully synthesized and characterized using various spectroscopic methods. The photophysicochemical properties of compounds **3bH₂Pc**, **Zn3b** and **In3b** were investigated in DMSO. Also, the effect of the central metal ion in the phthalocyanine ring on these properties was investigated. These measurements indicate that the Φ_d values of all synthesized Schiff base-substituted phthalocyanines are almost the same. In addition, it was observed that the presence of metal ions increased the singlet oxygen quantum yield. The combination of a heavy In atom and the substituent containing a conjugated Schiff base group increased the Φ_Δ value as expected. Inhibition of PET from the methoxy moiety to the Pc ring also increased the Φ_Δ value. The obtained results show that the newly synthesized imine-substituted metallophthalocyanines are efficient and convenient photosensitizers for PDT applications.

In conclusion, the present *in vitro* study demonstrated that imine-substituted metal-free and metallophthalocyanines exhibit distinct photodynamic activities depending on the presence of a central metal ion. All phthalocyanine derivatives showed negligible dark cytotoxicity at the selected concentration, confirming their biocompatibility under non-irradiated conditions. Upon light activation, phthalocyanine-mediated PDT significantly reduced cell viability and induced apoptotic cell death in PC3 cells.

This photodynamic effect was accompanied by a significant increase in intracellular ROS generation, with metallophthalocyanines, particularly **In3b**, inducing markedly higher ROS levels than the metal-free derivative. The enhanced ROS production correlated well with the observed reductions in cell viability and enhancements in total apoptosis, indicating that ROS-mediated oxidative stress plays a central role in the cytotoxic mechanism of phthalocyanine-mediated PDT.

These findings provide a strong foundation for further mechanistic investigations and future *in vivo* studies aimed at advancing phthalocyanine-based PDT strategies.

Conflicts of interest

There are no conflict of interest.

Data availability

The data supporting the findings of this study are available within the article and its supplementary information (SI). Supplementary information is available. See DOI: https://doi.org/10.1039/d6dt00397d.

Acknowledgements

References

1 R. L. Siegel, K. D. Miller, N. S. Wagle and A. Jemal, Cancer statistics, 2023, *CA Cancer J. Clin.*, 2023, **73**, 17–48, DOI: 10.3322/caac.21763.

2 G. Y. Atmaca, M. Aksel, M. D. Bilgin and A. Erdoğmuş, Comparison of sonodynamic, photodynamic and sonophotodynamic therapy activity of fluorinated pyridine substituted silicon phthalocyanines on PC3 prostate cancer cell line, *Photodiagn. Photodyn. Ther.*, 2023, **42**, 103339, DOI: 10.1016/j.pdpdt.2023.103339.

3 B. S. Bilen, M. Özçeşmeci, N. Koçyiğit, T. Elgün, A. G. Yurttaş and E. Hamuryudan, Glycosylated zinc(II) phthalocyanine photosensitizer: Synthesis, photophysical properties and in vitro photodynamic activity on breast cancer cell line, *J. Mol. Struct.*, 2024, **1295**, 136688, DOI: 10.1016/j.molstruc.2023.136688.

4 S. D. Ezquerra Riega, F. Valli, H. B. Rodríguez, J. Marino, L. P. Roguin, B. Lantaño and M. C. García Vior, Chalcogen bearing tetrasubstituted zinc(II) phthalocyanines for CT26 colon carcinoma cells photodynamic therapy, *Dyes Pigm.*, 2022, **201**, 110110, DOI: 10.1016/j.dyepig.2022.110110.

5 A. Crous, S. S. Dhilip Kumar and H. Abrahamse, Effect of dose responses of hydrophilic aluminium(III) phthalocyanine chloride tetrasulphonate based photosensitizer on lung cancer cells, *J. Photochem. Photobiol., B*, 2019, **194**, 96–106, DOI: 10.1016/j.jphotobiol.2019.03.018.

6 S. Zeinali, A. Tuncel, A. Yüzer and F. Yurt, Imaging and detection of cell apoptosis by photodynamic therapy applications of zinc(II) phthalocyanine on human melanoma cancer, *Photodiagn. Photodyn. Ther.*, 2021, **36**, 102518, DOI: 10.1016/j.pdpdt.2021.102518.

7 I. D. Burtsev, T. V. Dubinina, A. E. Egorov, A. A. Kostyukov, A. V. Shibaeva, A. S. Agranat, M. M. Ivanova, L. R. Sizov, N. V. Filatova, A. Y. Rybkin, E. V. Varakina, A. S. Bunev, A. A. Antonets, E. R. Milaeva and V. A. Kuzmin, Substituted boron subphthalocyanines – Prospective compounds for theranostics: Synthesis, photochemical properties and in vitro cytotoxicity, *Dyes Pigm.*, 2022, **207**, 110690, DOI: 10.1016/j.dyepig.2022.110690.

8 N. Nwahara, G. Abrahams, J. Mack, E. Prinsloo and T. Nyokong, A hypoxia responsive silicon phthalocyanine containing naphthoquinone axial ligands for photodynamic therapy activity, *J. Inorg. Biochem.*, 2023, **239**, 112078, DOI: 10.1016/j.jinorgbio.2022.112078.

9 B. Li, Z. Cui, Y. Han, J. Ding, Z. Jiang and Y. Zhang, Novel axially substituted lanthanum phthalocyanines: Synthesis, photophysical and nonlinear optical properties, *Dyes Pigm.*, 2020, **179**, 108407, DOI: 10.1016/j.dyepig.2020.108407.

10 G. Gümüşgöz Çelik, G. Tunç, F. Lafzi, N. Saracoglu, B. Seçkin Arslan, M. Nebioğlu, İ. Şişman and A. Gül Gürek, Influence of spacer and donor groups as tetraphenylethylene or triphenylamine in asymmetric zinc phthalocyanine dyes for dye-sensitized solar cells, *J. Photochem. Photobiol., A*, 2023, **444**, 114962, DOI: 10.1016/j.jphotochem.2023.114962.

11 G. Kocakülah, Comparison of electro-optical and dielectric properties of cobalt(II) phthalocyanine doped cholesteric liquid crystals, *Opt. Mater.*, 2023, **141**, 113949, DOI: 10.1016/j.optmat.2023.113949.

12 J. Zhang, F. Lu, H. Huang, J. Wang, H. Yu, J. Jiang, D. Yan and Z. Wang, Near infrared electrochromism of lutetium phthalocyanine, *Synth. Met.*, 2005, **148**, 123–126, DOI: 10.1016/j.synthmet.2004.09.027.

13 H. Wu, G. Liu, K. Chen, T. Zhang, Q. Ye, J. Chen and Y. Peng, A piperazine-substituted phthalocyanine with rapid cellular uptake and dual organelle-targeting for in vitro photodynamic therapy, *Photodiagn. Photodyn. Ther.*, 2023, **44**, 103818, DOI: 10.1016/j.pdpdt.2023.103818.

14 T. Sizun, M. Bouvet, Y. Chen, J.-M. Suisse, G. Barochi and J. Rossignol, Differential study of substituted and unsubstituted cobalt phthalocyanines for gas sensor applications, *Sens. Actuators, B*, 2011, **159**, 163–170, DOI: 10.1016/j.snb.2011.06.067.

15 J. Guo, X. Yan, Q. Liu, Q. Li, X. Xu, L. Kang, Z. Cao, G. Chai, J. Chen, Y. Wang and J. Yao, The synthesis and synergistic catalysis of iron phthalocyanine and its graphene-based axial complex for enhanced oxygen reduction, *Nano Energy*, 2018, **46**, 347–355, DOI: 10.1016/j.nanoen.2018.02.026.

16 Ü. Demirbaş, Novel peripherally tetra substituted phthalocyanines: Synthesis, characterization, photophysical and photochemical properties, *J. Mol. Struct.*, 2020, **1211**, 128082, DOI: 10.1016/j.molstruc.2020.128082.

17 I. D. Burtsev, Y. B. Platonova, A. N. Volov and L. G. Tomilova, Synthesis, characterization and photochemical properties of novel octakis(p–fluorophenoxy)substituted phthalocyanine and its gallium and indium complexes, *Polyhedron*, 2020, **188**, 114697, DOI: 10.1016/j.poly.2020.114697.

18 H. Yanık, D. Aydın, M. Durmuş and V. Ahsen, Peripheral and non-peripheral tetrasubstituted aluminium, gallium and indium phthalocyanines: Synthesis, photophysics and photochemistry, *J. Photochem. Photobiol., A*, 2009, **206**, 18–26, DOI: 10.1016/j.jphotochem.2009.05.005.

19 C. Biral Silva, F. C. Torres Antonio, P. Homem-de-Mello, A. O. Ribeiro and H. P. M. de Oliveira, Concentration and solvent effects, photochemical and photophysical properties of methyl and tert-butyl zinc(II) and aluminum(III) phthalocyanines, *J. Mol. Struct.*, 2021, **1246**, 131103, DOI: 10.1016/j.molstruc.2021.131103.

20 M. Pişkin, E. Canpolat and Ö.F Öztürk, The new zinc phthalocyanine having high singlet oxygen quantum yield substituted with new benzenesulfonamide derivative groups containing schiff base, *J. Mol. Struct.*, 2020, **1202**, 127181, DOI: 10.1016/j.molstruc.2019.127181.

21 P. Sen, J. Mack and T. Nyokong, Indium phthalocyanines: Comparative photophysicochemical properties and photodynamic antimicrobial activities against Staphylococcus aureus and Escherichia coli, *J. Mol. Struct.*, 2022, **1250**, 131850, DOI: 10.1016/j.molstruc.2021.131850.

22 S. Ünlü, F. T. Elmalı, G. Y. Atmaca and A. Erdoğmuş, Synthesis of phenanthroline substituted five-nuclear phthalocyanine zinc complex and exploring of photochemical and sono-photochemical properties, *Polyhedron*, 2024, **250**, 116817, DOI: 10.1016/j.poly.2023.116817.

23 G. Karanlık, C. Can Karanlık, G. Yaşa Atmaca and A. Erdoğmuş, Comparative evaluation of singlet oxygen

generation of new tetra-schiff base substituted zinc phthalocyanine by photochemical and sonophotochemical techniques, *J. Mol. Struct.*, 2024, **1299**, 137233, DOI: 10.1016/j.molstruc.2023.137233.

24 L. V. Gavali, A. A. Mohammed, M. J. K. Al-Ogaili, S. H. Gaikwad, M. Kulkarni, R. Das and P. A. Ubale, Novel terephthalaldehyde bis(thiosemicarbazone) Schiff base ligand and its transition metal complexes as antibacterial Agents: Synthesis, characterization and biological investigations, *Results Chem.*, 2024, **7**, 101316, DOI: 10.1016/j.rechem.2024.101316.

25 R. A. Ammar, A.-N. M. A. Alaghaz, M. E. Zayed and L. A. Al-Bedair, Synthesis, spectroscopic, molecular structure, antioxidant, antimicrobial and antitumor behavior of Mn(II), Co(II), Ni(II), Cu(II) and Zn(II) complexes of O 2 N type tridentate chromone-2-carboxaldehyde Schiff's base ligand, *J. Mol. Struct.*, 2017, **1141**, 368–381, DOI: 10.1016/j.molstruc.2017.03.080.

26 O. Gungor, A. Gul, S. Ali Gungor, S. Comertpay and M. Kose, Synthesis, DNA binding and anticancer properties of new Cu(II) and Zn(II) complexes of a Schiff base ligand containing a triphenylphosphonium as a lipophilic cation, *J. Photochem. Photobiol., A*, 2024, **450**, 115453, DOI: 10.1016/j.jphotochem.2023.115453.

27 C. Sarı, İ. Değirmencioğlu and F. C. Eyüpoğlu, Synthesis and characterization of novel Schiff base-silicon(IV) phthalocyanine complex for photodynamic therapy of breast cancer cell lines, *Photodiagn. Photodyn. Ther.*, 2023, **42**, 103504, DOI: 10.1016/j.pdpdt.2023.103504.

28 K. Harmandar, M. F. Saglam, I. F. Sengul, G. Ekineker, P. Balcik-Ercin, M. Göksel and D. Atilla, Novel triazole containing zinc(II)phthalocyanine Schiff bases: Determination of photophysical and photochemical properties for photodynamic cancer therapy, *Inorg. Chim. Acta*, 2021, **519**, 120286, DOI: 10.1016/j.ica.2021.120286.

29 H. Yanık, S. Y. Al-Raqa, A. Aljuhani and M. Durmuş, The synthesis of novel directly conjugated zinc(II) phthalocyanine via palladium-catalyzed Suzuki–Miyaura cross-coupling reaction and its quaternized water-soluble derivative: Investigation of photophysical and photochemical properties, *Dyes Pigm.*, 2016, **134**, 531–540, DOI: 10.1016/j.dyepig.2016.08.009.

30 C. Can Karanlık, G. Karanlık and A. Erdoğmuş, A Strategy for Increasing Singlet Oxygen Quantum Yield for Water–Soluble Distyryl–BODIPY Derivative, *Appl. Organomet. Chem.*, 2025, **39**, e70184, DOI: 10.1002/aoc.70184.

31 A. Günsel, A. T. Bilgiçli, B. Tüzün, H. Pişkin, G. Y. Atmaca, A. Erdoğmuş and M. N. Yarasir, Synthesis of tetra-substituted phthalocyanines bearing 2-(ethyl(m-tolyl)amino) ethanol: Computational and photophysicochemical studies, *J. Photochem. Photobiol., A*, 2019, **373**, 77–86, DOI: 10.1016/j.jphotochem.2018.12.038.

32 M. Syuleyman, I. Angelov, Y. Mitrev, M. Durmuş and V. Mantareva, Cationic amino acids linked to Zn(II) phthalocyanines for photodynamic therapy: Synthesis and effects on physicochemical properties, *J. Photochem. Photobiol., A*,

2020, **396**, 112555, DOI: 10.1016/j.jphotochem.2020.112555.

33 N. Kocaağa, A. Türkkol, M. D. Bilgin and A. Erdoğmuş, The synthesis of novel water-soluble zinc(II) phthalocyanine based photosensitizers and exploring of photodynamic therapy activities on the PC3 cancer cell line, *Photochem. Photobiol. Sci.*, 2023, **22**, 2037–2053, DOI: 10.1007/s43630-023-00428-y.

34 M. Pişkin, Phthalocyanine photosensitizers with bathochromic shift, of suitable brightness, capable of producing singlet oxygen with effective efficiency, *J. Photochem. Photobiol., A*, 2023, **435**, 114325, DOI: 10.1016/j.jphotochem.2022.114325.

35 M. Pişkin, The novel 2,6-dimethoxyphenoxy substituted phthalocyanine dyes having high singlet oxygen quantum yields, *Polyhedron*, 2016, **104**, 17–24, DOI: 10.1016/j.poly.2015.11.017.

36 X.-F. Zhang and N. Feng, Attaching naphthalene derivatives onto BODIPY for generating excited triplet state and singlet oxygen: Tuning PET-based photosensitizer by electron donors, *Spectrochim. Acta, Part A*, 2018, **189**, 13–21, DOI: 10.1016/j.saa.2017.08.005.

37 A. Ogunsipe, D. Maree and T. Nyokong, Solvent effects on the photochemical and fluorescence properties of zinc phthalocyanine derivatives, *J. Mol. Struct.*, 2003, **650**, 131–140, DOI: 10.1016/S0022-2860(03)00155-8.

38 C. Can Karanlık and A. Erdoğmuş, The ultrasound and light combination as a new approach for BODIPY dyes with the enhanced singlet oxygen formation, *J. Photochem. Photobiol., A*, 2024, **447**, 115210, DOI: 10.1016/j.jphotochem.2023.115210.

39 B. Sajjadifard, H. P. Karaoğlu, C. C. Karanlık, A. Erdoğmuş, M. S. Yalçın, S. Özdemir and A. K. Burat, π-Conjugated fluorenyl-based phthalocyanines: Synthesis, photophysical, photochemical properties, and biological evaluation, *Dyes Pigm.*, 2026, **246**, 113357, DOI: 10.1016/j.dyepig.2025.113357.

40 Ö.D Kutlu, A. Erdoğmuş, P. Şen and S. Z. Yıldız, Peripherally tetra-Schiff base substituted metal-free and zinc(II) phthalocyanine, its water-soluble derivative: Synthesis, characterization, photo-physicochemical, aggregation properties and DNA/BSA binding activity, *J. Mol. Struct.*, 2023, **1284**, 135375, DOI: 10.1016/j.molstruc.2023.135375.

41 M. Yüzeroğlu, G. Keser Karaoğlan, G. Gümrükçü Köse and A. Erdoğmuş, Synthesis of new zinc phthalocyanines including schiff base and halogen; photophysical, photochemical, and fluorescence quenching studies, *J. Mol. Struct.*, 2021, **1238**, 130423, DOI: 10.1016/j.molstruc.2021.130423.

42 G. Karanlık, C. Can Karanlık and A. Erdoğmuş, Investigation of sonophotochemical effectiveness of Schiff-base decorated novel silicon(IV) phthalocyanines with heteroaromatic moiety, *J. Mol. Struct.*, 2025, **1346**, 143223, DOI: 10.1016/j.molstruc.2025.143223.

43 H. Yalazan, İ. Ömeroğlu, M. Durmuş and H. Kantekin, 4-Aminoantipyrine-derived Schiff base substituted novel sym-

metrical zinc(II) phthalocyanine photosensitizers: Design, synthesis, photophysical, and photochemical properties for photodynamic therapy of cancer, *Inorg. Chem. Commun.*, 2025, **181**, 115125, DOI: 10.1016/j.inoche.2025.115125.

44 T. Nyokong, Effects of substituents on the photochemical and photophysical properties of main group metal phthalocyanines, *Coord. Chem. Rev.*, 2007, **251**, 1707–1722, DOI: 10.1016/j.ccr.2006.11.011.

45 C. C. Karanlık, G. Karanlık, B. Gok, Y. Budama-Kilinc, S. Kecel-Gunduz and A. Erdoğmuş, Exploring anticancer properties of novel Nano-Formulation of BODIPY Compound, Photophysicochemical, in vitro and in silico evaluations, *Spectrochim. Acta, Part A*, 2023, **301**, 122964, DOI: 10.1016/j.saa.2023.122964.

46 Ö. Özten, C. Adkuvayçin, C. C. Karanlık, F. Aguilar-Galindo, M. Z. Yıldız, L. Sobotta, A. Erdoğmuş and E. Güzel, Potential zinc phthalocyanine-based photosensitizer for photodynamic therapy: Photophysical, theoretical and in vitro studies, *J. Inorg. Biochem.*, 2025, **270**, 112958, DOI: 10.1016/j.jinorgbio.2025.112958.

47 B. Akkoç, T. Samsunlu, Ş. Işık, M. Özçeşmeci, G. Y. Atmaca, A. Erdoğmuş, M. Serhatlı and E. Hamuryudan, Pegylated metal-free and zinc(II) phthalocyanines: synthesis, photophysicochemical properties and *in vitro* photodynamic activities against head, neck and colon cancer cell lines, *Dalton Trans.*, 2022, **51**, 10136–10147, DOI: 10.1039/D2DT00704E.

48 M. Serhatli, S. Isik, A. Kalkan, M. Özçeşmeci, E. Hamuryudan and Ö. Can, Morpholinoethoxy-Substituted Cationic Metal-Free and Metallo Phthalocyanines: In Vitro Photodynamic Therapy Activities, PDT-Induced ROS Level Measurements, and Cellular Death Mechanism, *ACS Bio Med Chem Au*, 2025, **5**, 766–777, DOI: 10.1021/acsbiomedchemau.5c00137.

49 N. W. Nkune, G. G. Matlou and H. Abrahamse, Photodynamic Therapy Efficacy of Novel Zinc Phthalocyanine Tetra Sodium 2-Mercaptoacetate Combined with Cannabidiol on Metastatic Melanoma, *Pharmaceutics*, 2022, **14**, 2418, DOI: 10.3390/pharmaceutics14112418.

50 E. Güzel, G. Y. Atmaca, A. E. Kuznetsov, A. Turkkol, M. D. Bilgin and A. Erdoğmuş, Ultrasound versus Light: Exploring Photophysicochemical and Sonochemical Properties of Phthalocyanine-Based Therapeutics, Theoretical Study, and In Vitro Evaluations, *ACS Appl. Bio Mater.*, 2022, **5**, 1139–1150, DOI: 10.1021/acsabm.1c01199.